CONSIDERATION OF SOLAR RADIATION IN FLARE DESIGN

A Thesis

by

ANKITA TANEJA

Submitted to the Office of Graduate and Professional Studies of
Texas A&M University
in partial fulfillment of the requirements for the degree of

MASTER OF SCIENCE

Chair of Committee,	M. Sam Mannan
Committee Members,	Mahmoud El-Halwagi
	Sharath Girimaji
Head of Department,	M. Nazmul Karim

May 2018

Major Subject: Chemical Engineering

ABSTRACT

At oil refineries and other chemical processing plants, a flare stack is used to get rid of unwanted or excessive gases and relieve the system of excess pressure. These gases can be generated during different stages of operation like startup or shutdown, maintenance and process upsets. Since flares handle large amounts of toxic and flammable materials, it makes the flaring operation hazardous. Combustion of huge amount of gases releases heat which is radiated to the atmosphere. Heat radiated from the flare makes it important for siting the flare at a proper location. The heat radiation should not exceed recommended threshold levels so that people on-site and the equipment are not affected. Thus, to have a well-designed flare, knowledge of total radiation emitted from a flare is essential. It will aid in accurately estimating the flare height and the area near the flare, which would sustain high levels of thermal radiation.

A common point of contention while calculating radiation level emitted from flare is the decision of including solar radiation (SR) in the calculations. API 521 relegates this decision to the flare design company's practices. Based on expert judgement, some literature states that for all practical purposes, solar radiation contribution can be discounted.

The work performed aims at presenting a framework which quantitatively addresses aforementioned obscurity. The analysis helps flare designers to more objectively decide whether to include SR in their analyses or treat it insignificant contribution. The work studies the various factors that cause variation in SR value:

location, time, and orientation of the surface. Considering all these parameters, an appropriate value of SR is chosen as the solar contribution to the thermal radiation from the flare. The effect of SR to the design of the flare is quantified by studying the change in effect distance near the flare and the height of the flare. Consequence analysis software PHAST is used to obtain these calculations. In addition, the outcome that SR inclusion will have on the risk posed by the flare due to thermal radiation on personnel is also examined. This is studied by measuring the change in lethality and heat stress caused by radiation exposure.

DEDICATION

To my mother Ranjana Taneja and my father Shanker Taneja for their unconditional love and support in every decision I have taken. To my little sister Drishti Taneja for bringing immense joy in my life.

ACKNOWLEDGEMENTS

I want to firstly thank my research advisor Dr. M. Sam Mannan for all his support and feedback throughout my study. His dedication to the Mary Kay O' Connor Process Safety Center and process safety at large has continued to inspire me.

I would like to thank my committee members, Dr. Mahmoud El-Halwagi and Dr. Sharath Girimaji for their guidance and support throughout the course of this research.

I want to appreciate the time devoted by Dr. Delphine Laboureur, Dr. Hans Pasman and Dr. Bin Zhang in providing guidance for my research.

Thanks also go to my friends Kunal Das, Nikhil Mayadeo and Nilesh Ade for being there in need and helping me in all ways they could.

I also thank the department faculty and staff for making my time at Texas A&M University a great experience.

I am forever grateful to my mother, father and sister for showering their love and being my life's inspiration.

.

CONTRIBUTORS AND FUNDING SOURCES

Contributors

This work was supported by a thesis committee consisting of Professor M. Sam Mannan of the Department of Chemical Engineering, Professor Mahmoud-El Halwagi of the Department of Chemical Engineering and Professor Sharath Girimaji of the Department of Ocean Engineering.

The work conducted for this thesis was completed by the student independently.

Funding Sources

Graduate study was supported by Chemical Engineering Award from Department of Chemical Engineering, Texas A&M University. TX Public Education Grant from the state of Texas and Harry West Memorial Endowment from Mary Kay O'Connor Process Safety Center at Texas A&M University was also awarded to support graduate study.

TABLE OF CONTENTS

Page

LIST OF FIGURES

Page

LIST OF TABLES

Page

1 INTRODUCTION

Industrial flares are used as part of the safety and pollution control systems in industries that handle hydrocarbons, like, the oil & gas and the petrochemical industries. The material sent to the flare is predominantly light hydrocarbon gases where they undergo combustion. A flare stack is used to get rid of unwanted or excessive gases. These gases can be generated during different stages of operation like startup or shutdown, maintenance and process upsets. Off-spec products and bypass streams are also sometimes sent to the flare. All viable efforts are made to recycle the gas or recover its waste heat before sending it to the flare stack, but this is not feasible on all occasions. Therefore, gas flaring is utilized as the last in line of defense in relieving the system of excess pressure. Devices like rupture discs, pressure relief and blowdown valves are used to direct the waste gas to the flaring system. These pressure relief devices are connected to a header that collects the released vapor and sends it to a flare for combustion.

In older times, the waste gas vented from pressure relieving equipment was released directly into the atmosphere. Only in the late 1940s, when the awareness towards environment protection grew, industrial flare started to see its usage as a system where waste gases were collectively burned (Baukal Jr, 2012c). This method of disposal of the vapors and sometimes liquids is a more environmentally friendly option. The gases flared are generally flammable, toxic, and/or corrosive. Their direct discharge to the environment in excess of the explosion/toxic threshold limit can put the plant

personnel, the general public around the facility, and the surrounding equipment in danger. By carrying complete combustion of the gases, they are converted to lesser hazardous substances: carbon dioxide and water vapor.

On the basis of elevation, flares can be classified into categories of elevated or ground-level flares (Banerjee, Cheremisinoff, & Cheremisinoff, 1985). Ground flare, as the name suggests, carries the combustion process on the ground, making the installation and maintenance of the system relatively cheaper. The problem of excessive glare, which might be a considerable issue for the public living near the facility, can also be eliminated if the flare is enclosed. For elevated flares, burners and igniters are located at the top of the stack, because of which the pollutant concentration and the thermal radiation experienced on the ground is much lesser. They also require less space and need not be as isolated from the rest of the plant due to the same reason.

Another basis of distinction of flares is whether the flare is assisted or non-assisted. The flow of the gases to the burner can be improved by using air/steam as an assist. It also helps in better mixing of the fuel and air by improving air entrainment, which results in smokeless burning and higher destruction efficiency.

The fact that the flare system handles large amounts of hazardous material makes the flaring operation hazardous. Some of the key design factors that play a significant role in ensuring safe and smooth flare operation are:

- Superior combustion efficiency and near smokeless emission
- No liquid carryover to the flare tip
- Vibration and noise level

- Thermal radiation

In this study, flare design is examined in terms of thermal radiation as a design factor. Combustion of huge amount of gases at the flare releases heat which is radiated to the atmosphere. Even when the flare is elevated, thermal radiation can cause harm without requiring contact with the fire/hot surface by virtue of the elevated temperature. Heat radiated from the flare is important for siting flare at a proper location. Hence, thermal radiation is recognized as a very crucial requirement for ensuring safe operation. The heat radiation should not exceed recommended threshold level so that the people on-site and the equipment are not affected. This is the reason for the flare to be generally placed at an isolated location or where the prevalent wind direction directs the flame away from the facility.

Thus, to have a well-designed flare, knowledge of total radiation emitted from a flare is important to be known. It will aid in accurately estimating the flare height and the area near the flare which would sustain high level of thermal radiation. When calculating total radiation from flare, the radiation from the sun should also be accounted for to accurately predict thermal radiation levels. However, this idea is not free from debate and will be discussed in further sections.

2 LITERATURE REVIEW

An adequately designed flare should be able to dispose the unwanted gases efficiently and in an environmentally acceptable fashion while being economically feasible. The objective of designing a flare system properly is achieved by taking into account various design considerations, for example, dependable and clean combustion, avoiding liquid carryover from waste stream to the flare stack, amount of noise, glare and thermal radiation generated. These considerations are briefly described in the following paragraphs.

The flare serves the important role of destroying the flammable and toxic gases before it is released to the environment. Title 40 of the Code of Federal Regulation §60.18 prescribes the various operating conditions for flares. It states that a pilot flame should be burning throughout at the top end of the flare stack. It also restricts the facility to only have smokeless burning or emit smoke for a maximum of five minutes during two hours of operation. Smoke is generated due to incomplete combustion of a fuel-rich gas, *i.e.*, adequate amount of oxygen is required to avoid smoke. If gases have a higher exit velocity, better fuel-air mixing is achieved. This is because higher momentum of the gas ingresses more air into the mixture. Therefore, federal regulations control the velocity of exit gases from the flare to avoid burning of hydrocarbons along with smoke emission.

It is very important to remove any liquid droplets from the waste stream before it is sent to the flare stack. The stack is not designed to handle liquids. Any liquid burning

at the flare tip will generate soot and cause environmental pollution. API 521 (2007) suggests removing droplets of a size larger than 300-600 μm in the knockout drum installed before the flare stack. This is done to avoid "flaming rain" emanating from the flare tip.

Since flare stack handles large amount of hydrocarbon vapors, sometimes as much as 10^6 lb/hr (Baukal Jr, 2012a), a lot of noise is produced from its operation. Noise produced from the flare is of two types: combustion roar and gas jet noise (Baukal Jr, 2012b). Isolating the source of noise by increasing the flare height is not a feasible option because noise levels do not drop significantly in the area of operation by secluding the origin. Thus, more efforts are put in mitigating the problem. Most common of them is the method of reducing the noise as it traverses from the source to the receiver. Silencers and mufflers are widely used for this purpose (Baukal Jr, 2012b).

Furthermore, flare radiation has been recognized as one of the important elements of flare system design criteria. Burning of waste gases at elevated temperature generates intense heat. Some of this heat is transferred to the surroundings in the form of thermal radiation. The radiation can adversely affect people that might be exposed. The effects can be physiological, like increase in heart beat rate, excessive sweating and elevated temperature of the body. But, these aspects come into picture only if the exposure is extended. The pathological effects, that are much more predominant, can lead to various degrees of skin burn and even prove to be fatal (Bosch & Twilt, 1992). Thermal radiation can also impact the equipment installed nearby. It can weaken the material, depending on the length and intensity of exposure. It can also escalate the

temperature of the process stream inside the vessel, potentially increasing the interior pressure and causing a rupture or leak. Considering these factors, knowledge of accurate levels of thermal radiation at the ground level is crucial for: deciding the restricted area near the flare where radiation would be too high, and the height of the flare stack in case of elevated flares. It will also be helpful in knowing the risk associated with thermal radiation exposure for the personnel working near the flare.

The American Petroleum Institute (API) releases widely recognized standards and guidelines for the oil and gas industry. API 537 (2008) is written to aid the mechanical design and operation of flare system and its components. API 521 (2007) is the companion document providing guidelines for the design of flare stack constituents like, the flare burner, flare tip and auxiliary components like liquid seal or knockout drum.

One of the requirements that a flare must meet, is the amount of thermal radiation that can be experienced by the personnel and the equipment. API 521 suggests using the method developed empirically by Hajek and Ludwig in calculating thermal radiation (Hajek & Ludwig, 1960):

$$D = \sqrt{\frac{F.\tau.Q}{K.4\pi}} \quad (1)$$

D distance of the desired location measured from the assumed center of flare (m or ft.)

F ratio of energy transfer by radiation to the total energy generated

τ atmospheric transmittance

Q heat liberated (kW or Btu/hr)

K radiation intensity level at distance D (kW/m^2 or Btu/hr.ft^2)

Many authors (Chamberlain, 1987; Oenbring & Sifferman, 1980) have presented their work showing theoretical and empirical methods to calculate F, fraction of heat radiated. It is shown that F is dependent on factors like flame geometry, view factor of the receiving surface and gas velocity at exit. Transmissivity, τ depends on atmospheric conditions, like cloud cover, ambient temperature, and humidity.

The model presented above is more commonly called the single-point model, due to the assumption that all the heat is radiated from a single point located somewhere near the center of the flare. It gives accurate results for far-field but has shown higher deviation for distances closer to the fire.

Many other models have been developed thereafter, most of them assume the flare to be a solid body radiating heat from its entire surface (Chamberlain, 1987; Johnson, Brightwell, & Carsley, 1994). The validation of these models against experimental data shows that it gives better prediction of radiation intensity even in the near-field region.

API 521 (2007) recommends thermal radiation flux density levels, K, for flare design purposes as shown in Table 1. These levels are chosen based on specific operating conditions of the facility. A higher radiation level, K is chosen for a greater volume of fluid release from the flare, lasting for a short span of time, *i.e.*, in case of emergency flaring operation, and should also reflect in a short exposure time for personnel. On the other hand, a lower radiation level is chosen for a prolonged release of

relatively low volume of fluid burned at the flare as in the case of normal operation of flare.

API 521 mentions that consideration of radiation from the sun in calculating the thermal radiation level is discretionary upon the flare design company. Since, the value of solar radiation is said to be in the range of 0.79-1.04 kW/m^2, this adjustment to the thermal radiation level might not yield significant difference for higher radiation levels of 6.31 kW/m^2 and up.

Table 1. Suggested Thermal Radiation for People Exposed

Acceptable radiation for design, *K* kW/m^2 (Btu/hr.ft^2)	**Condition**
9.46 (3000)	Maximum radiation level for the area where personnel can perform desperate emergency activity. Radiation above 6.3 kW/m^2 requires protective gear to be worn.
6.31 (2000)	Maximum radiation level for the area where personnel can perform emergency activity for 30 seconds wearing suitable clothing and not requiring shielding.
4.73 (1500)	Maximum radiation level for the area where personnel can perform emergency activity for about 2-3 minutes wearing suitable clothing and not requiring shielding.
1.58 (500)	Maximum radiation level for the area where personnel wearing suitable clothing may be exposed steadily.
Suitable clothing comprises of full sleeve shirt, full pants, hard hat, shoes, and gloves.	

John Zink Combustion Handbook is a rich source of information about all the aspects of flare design, including but not limited to: equipment specification, critical design factors, environmental concerns, and safety considerations (Baukal Jr, 2012d). It recognizes radiation emanated from the flare as a crucial design factor for facility layout. Solar radiation accommodation to the thermal radiation level is a point of divisiveness and is seen to vary from operator to operator. It has been pointed out that more often than not, solar radiation can be safely ignored (Schwartz & Kang, 1998). Nevertheless, the decision is location dependent and also, specific to the safety level desired.

However, there are some resources which suggest otherwise. They point towards the importance of including solar radiation when predicting thermal radiation level for design of flare system (Baukal Jr, 2012d). Its effect on the design can be seen by observing change in length of flare boom in case of a platform or change in height of flare for an onshore site. The factor causing the most variation in the amount of radiation intensity received by the earth: the time of the year, is also discussed. Results are presented for solar radiation received on a surface either oriented normal to the incoming sunlight or parallel to the ground at Tulsa, OK. It is clearly seen that the radiation intensity on a horizontal plane varies widely for different months of the year.

A case where the decision of considering or discounting solar radiation becomes even more critical, is that of an offshore platform/vessel (McMurray, Oswald, & Witheridge, 1980). Under-design in terms of exceeding thermal radiation levels can have dire consequences, especially for some of the critical areas, like: drilling derrick and entryway to the life-boats. Personnel are either present in these areas for a couple of

hours, or they are used in case of an emergency. A platform has a very limited area leaving no possibility for workers to escape to a location with lesser radiation level, in case of under-design. In contrast, overestimation of the radiation level will lead to a more conservative design in terms of taller flare stack. This will result in a more expensive and heavier structure. Over-design can also lead to greater exclusion zone, thus taking more of the already limited space on a platform. In addition, this study also identifies that considering maximum value of solar radiation and simply adding it to the radiation from flare would lead to gross over-design. The study also mentions that the concept of likelihood of worst conditions occurring be given some thought. It compares the design of flare, with and without solar radiation contribution corresponding to the case of calm weather and strong winds. The idea behind neglecting solar radiation in case of windy conditions is that convective cooling dominates over radiative heating.

A recapitulation of the literature review shows that the decision of making the solar radiation adjustment to the thermal radiation emanated from flare is not straightforward. There exist conflicting opinions in the literature and more in-depth analysis should be performed for a more accurate and at the same time, a more feasible solution.

3 STUDY OBJECTIVES

The intent of the work performed here was determined after identifying the lack of consensus that exists on consideration of radiation from the sun while estimating thermal radiation emanated from a flare. The primary objective of this study is to develop a framework for the assessment of solar radiation contribution to the design of a flare system. It should be noted here that the flare design is studied solely from the point of view of thermal radiation among all other factors that affect the design criteria.

To develop the framework mentioned above, the study is geared towards achieving following objectives:

- Analyze different factors that impact the value of solar radiation, *e.g.*, geometry of Earth and Sun, geographical location, orientation of surface.
- Study a model which incorporates the above-mentioned factors and is enabled to provide solar radiation values in an uncomplicated way. The model will facilitate in choosing an appropriate value that will serve as the contribution to thermal radiation from the Sun.
- Utilize a consequence analysis tool, PHAST by DNV-GL to calculate thermal radiation emitted by an elevated flare whose initial design conditions are assumed to be that of a typical flare.
- Quantitatively measure the outcome of considering/discounting solar radiation contribution to thermal radiation calculations from flare by assessing the change caused to certain design conditions; *e.g.*, effect

distance and height of the flare; and the change in the amount of risk posed to workers when exposed to thermal radiation. The risk is measured in terms of probability of death/second degree burns and in terms of heat stress caused by working for extended periods of time.

4 METHODOLOGY

As emphasized already, total radiation experienced on the ground level is a crucial design factor for flare system and its design specifications. The total radiation includes both thermal radiation emanated from the flare and the radiation from the sun. Therefore, the methodology to develop a flare design based on heat radiation requires inclusion of radiation both from flare and the sun. The radiation from sun is calculated using the clear-sky solar radiation model (ASHRAE Standard Committee, 2013) developed by American Society of Heating, Refrigerating and Air-Conditioning Engineers (ASHRAE) and the radiation from flare is calculated using semi-empirical models already built in consequence and process hazard analysis software, PHAST developed by DNV GL. Both these components are explained in detail below.

4.1 SOLAR RADIATION CALCULATION

Radiation received from the sun has three components: direct, diffuse and reflected. The total solar radiation at a surface is the summation of these three components. Direct or the beam radiation is comprised of the solar rays traveling in straight lines and reaching the surface. The part of the sunlight that gets scattered in the atmosphere due to the presence of suspended particles or other molecules is called diffuse radiation. Reflected radiation are those solar rays that gets reflected from non-atmospheric objects and the ground. The reflected radiation is quite low as compared to direct and diffuse radiation for most of the surfaces except for the case when snow is present. Snow reflects 80-90% of radiation striking its surface. The amount of radiation

getting distributed among these three components is dependent on the location, the terrain and the time of the observation. Also, calculation of solar radiation on a surface requires knowledge of the Earth-Sun geometry, geographic location and its orientation. These factors are described in detail below.

4.1.1 EARTH-SUN GEOMETRY

Since the Earth is tilted on its axis, the equator forms an angle with the rays coming from the Sun. This angle is called the declination angle, δ. Also, due to revolution of Earth around the Sun, declination angle varies with each passing day. It can be expressed by equation (2) (Cooper, 1969):

$$\delta = 23.45\ sin\left(360° \frac{n + 284}{365}\right) \tag{2}$$

All angles in the document are in degrees unless otherwise stated.

n is the day number, *e.g.*, for January 1, n = 1

The position of the Sun in the sky is represented by apparent solar time (AST). This is what is measured by a sundial. However, the time shown by a clock is the mean solar time. Since, the Earth moves around the Sun with varying velocity through the year, AST and mean solar time differ slightly. This difference is given by Equation Of Time (EOT) (Iqbal, 1983).

$$EOT = 2.2918[0.0075 + 0.1868\cos\Gamma - 3.2077\ sin\Gamma - 1.4615\cos(2\Gamma) - 4.089\sin(2\Gamma)] \tag{3}$$

where, EOT is in minutes, and

$$\Gamma = \frac{360^0}{365}\ (n - 1) \tag{4}$$

To obtain AST from local time, it must be adjusted for EOT and the time difference between the local meridian and the standard meridian for that location. AST can be calculated using the formula (ASHRAE Standard Committee, 2013):

$$AST = LST + \frac{EOT}{60} + \frac{LON - LSM}{15} \quad (5)$$

LST is the local standard time, in decimal hours and adjusted for daylight saving time

LON is the longitude of the location, degrees East (°E) of prime meridian (LON would be negative if located west of prime meridian)

LSM is the local standard meridian of the location, °E of prime meridian (LSM would be negative if located west of prime meridian)

It is important to know the position of the Sun before calculating how much radiation reaches the Earth. The position can be uniquely determined by knowing the solar altitude angle β, and the solar azimuth angle, φ. Solar altitude β corresponds to how high the sun is in the sky. It is the angle between the horizontal plane and the beam of sunlight. When the sun is rising or setting, β is 0° and is close to 90° at noon. It can be calculated using equation 6. Solar azimuth Φ is the angle between geographical South and a shadow casted on the ground by a vertical rod. Or, it can be thought of as an angle between the projection of a sunbeam on the horizontal plane and the geographical south. This report follows the convention of taking its value to be positive after noon and negative before noon. Both these angles are shown in Figure 1.

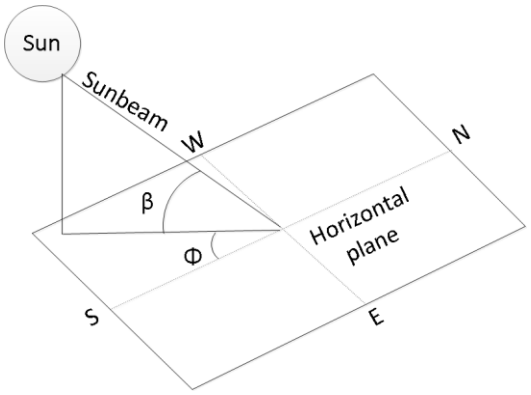

Figure 1. Solar altitude angle β, and solar azimuth angle, φ

Concepts of spherical trigonometry can be used to derive equations for β and φ (Kreith & Kreider, 1978) and are presented in equations 6 and 7 .

$$sin\beta = cosL\ cos\delta\ cosH + sinL\ sin\delta \tag{6}$$

$$sin\varphi = \frac{sinH\ cos\delta}{cos\beta} \tag{7}$$

where, L is the latitude of the location, positive for northern hemisphere and negative for southern hemisphere

H is the hour angle, in degrees, given by equation 8:

$$H = 15(AST - 12) \tag{8}$$

Ratio of the mass of air in the path of sunlight to earth to the mass of air in the path of sunlight to earth when the sun is precisely overhead is termed as air mass, m. It can be calculated using equation 9 (Kasten & Young, 1989):

$$m = \frac{1}{0.50572(\beta + 6.07995)^{-1.6364} + sin\beta} \tag{9}$$

4.1.2 SOLAR RADIATION MODEL

The solar radiation model presented here requires knowledge of radiation emitted by the Sun. Solar constant, E_{sc} represents the value of radiation on a plane at right angles to the sunrays placed at an average Sun-Earth distance. The widely accepted value of E_{sc} is 1367 W/m^2 (Iqbal, 1983). Since, the orbit of the Earth around the sun is elliptical, the actual radiation intensity received on a perpendicular plane before entering the Earth's atmosphere is not constant. It is more during winter months, when the Earth is closer to the Sun and lesser during summer months, when the Earth is farther. It can be calculated using the equation 10 (ASHRAE Standard Committee, 2013)

$$E_0 = \left(0.033\, cos\left(\frac{360^0}{365}\,(n-3)\right)+1\right)E_{sc} \qquad (10)$$

Using plethora of meteorological data from weather stations and sensors based on ground or space around the world, REST2 model was developed that predicts broadband solar irradiance for almost any location (Gueymard, 2008) . To have a simplified way of predicting beam and diffuse radiation from the sun, the model was parametrized. Consequently, only two parameters, unique to the location are used to predict the radiation values. These parameters are called beam and diffuse pseudo-optical depths, τ_b and τ_d, respectively. They are tabulated for more than 6,000 locations around the world for every 21st day of the month in the ASHRAE Handbook of Fundamentals (2013). Table 2 lists these values for Houston. However, for accurate calculation of radiation intensity, these values are required for each day of the year. Hence, the values for days other than the 21st day of the month, are interpolated using

the values from Table 2. The variation of τ_b and τ_d, with different days of the year is shown in Figure 3 and Figure 4 respectively.

It must be kept in mind that this model is developed for clear skies. It does not consider the effect of cloud cover on the amount of radiation reaching the Earth's surface. Among other atmospheric conditions, the cloud cover presents one of the highest variability in predicting radiation (Bamber & Payne, 2004). Hence, to reduce complexity, cloud cover has been left out of consideration. Nevertheless, this will give a more conservative estimate of the actual value of radiation.

Equations 11 and 12 represent the parametrization of the sophisticated broadband model, REST2. These are used to calculate the direct and the diffuse component of solar radiation.

$$E_b = E_0 \, e^{-\tau_b m^{ab}} \tag{11}$$

$$E_d = E_0 \, e^{-\tau_d m^{ad}} \tag{12}$$

here, E_b is direct component of radiation, also called beam radiation, measured at right angles to the incoming sunrays

E_d is diffuse component of radiation, measured on a horizontal surface

E_0 is extraterrestrial radiation as calculated in equation 10

τ_b and τ_d are beam and diffuse pseudo optical depths, unique to the location and tabulated for 21st day of each month; rest of the values are calculated by linear interpolation and shown in Figure 3 and Figure 4

m is the air mass as calculated in equation 9

ab and *ad* are the air mass exponents for beam component and diffuse component respectively, can be calculated using equations 13 and 14

$$ab = 1.219 - (0.043\tau_b + 0.151\tau_d + 0.204\tau_b\tau_d) \quad (13)$$

$$ad = 0.202 - (0.852\tau_b + 0.007\tau_d + 0.357\tau_b\tau_d) \quad (14)$$

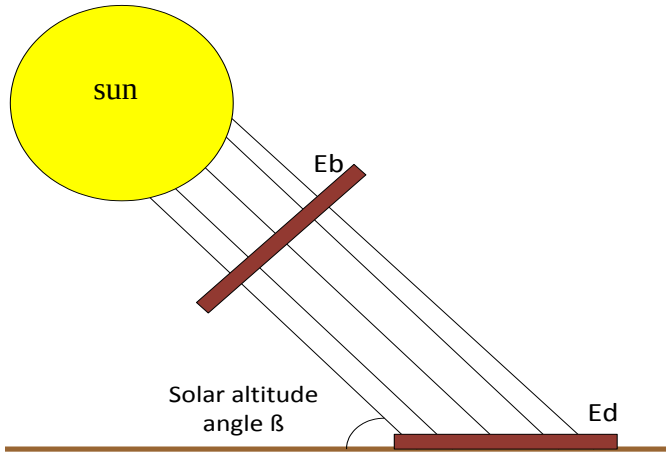

Figure 2. Depiction of direct and diffuse solar radiation

Table 2. Tabulated values of τ_b, τ_d for Houston for 21st day of each month

21st day of	Jan	Feb	Mar	Apr	May	Jun	Jul	Aug	Sep	Oct	Nov	Dec
τ_b	0.361	0.374	0.370	0.393	0.379	0.383	0.399	0.400	0.397	0.370	0.386	0.365
τ_d	2.562	2.487	2.447	2.344	2.384	2.404	2.381	2.404	2.442	2.529	2.489	2.561

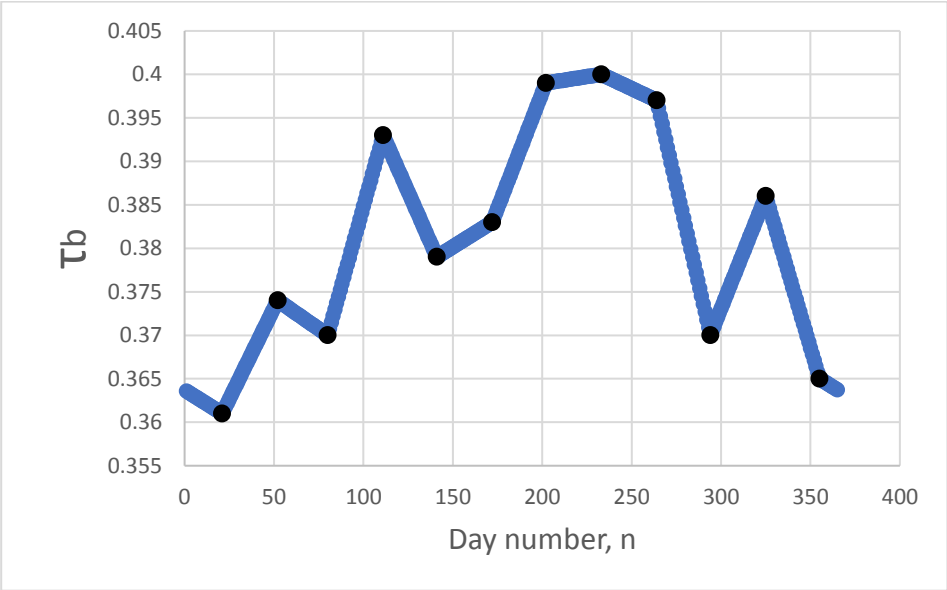

Figure 3. Variation of τ_b with day number, n

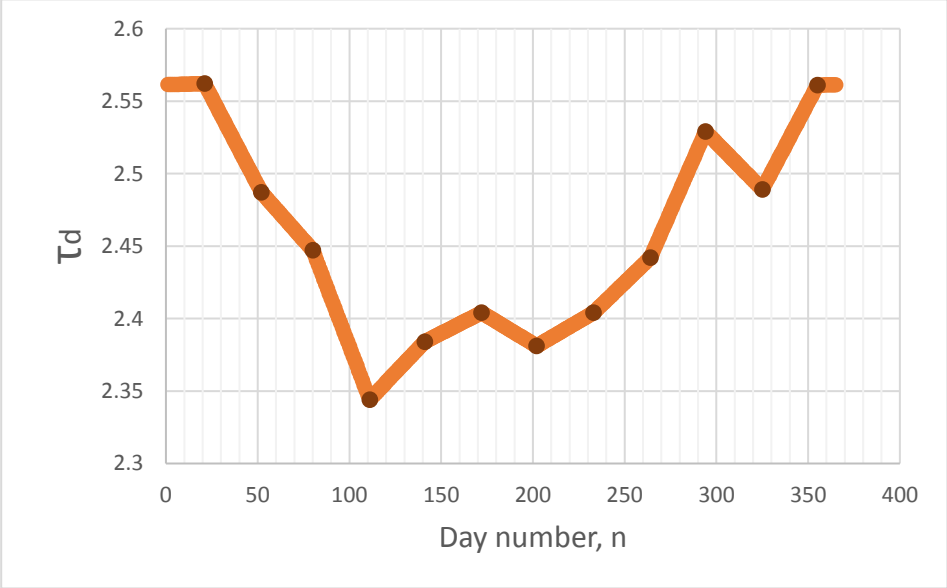

Figure 4. Variation of τ_d with day number, n

4.1.3 CALCULATION OF RADIATION FOR DIFFERENT ORIENTATION OF SURFACE

The values of radiation from the sun calculated from equations 11 and 12 are done only for two orientations of the surface, either perpendicular to the sunbeam or parallel to the ground. For designing a flare system according to the radiation exposure experienced by personnel on the ground, it is imperative to calculate the radiation level for the exposed people's orientation. For all practical purposes, the person can be assumed to be a vertical flat surface.

Orientation of a surface can be uniquely determined by knowing two quantities, the tilt angle Σ, and the surface azimuth angle ψ. They are shown in Figure 5 for a vertical surface.

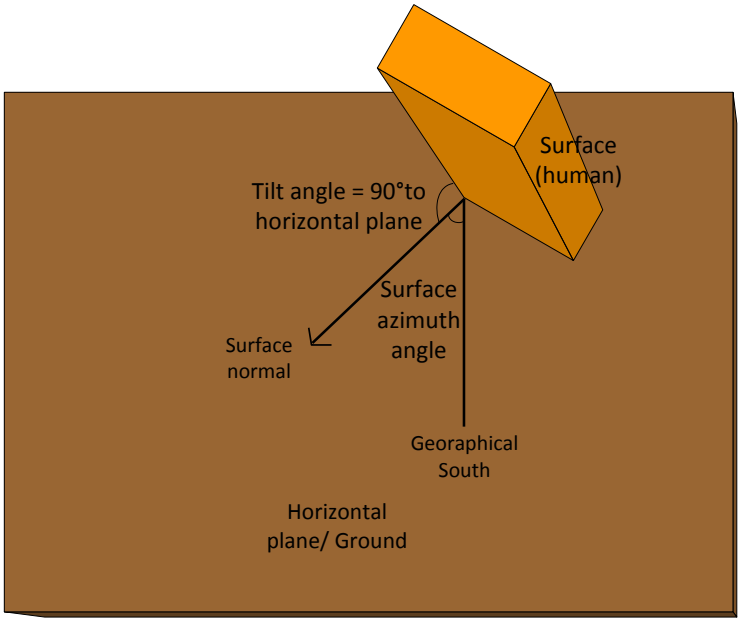

Figure 5. Tilt angle and azimuth angle for a vertical surface

The tilt angle Σ is the angle between the horizontal and the surface. It can vary from 0° to 180°, *e.g.*, a vertical surface will have a tilt angle of 90°. Surface azimuth angle ψ is the angle between the geographical south and the projection of the surface normal on the horizontal plane. By convention, angle measured clockwise from the South direction is positive and is negative for the anti-clockwise direction. For example, a surface facing West has ψ = 90° and a surface facing East has ψ = -90°.

Another angle used to represent the geometry of a surface with respect to the Sun is the surface-solar azimuth angle γ, which is the difference of solar azimuth angle φ (calculated from equation 7) and surface azimuth angle ψ discussed above, *i.e.*,

$$\gamma = \varphi - \psi \tag{15}$$

Lastly, the angle between the surface normal and the sunbeam is called the incidence angle θ which can be calculated using the following formula:

$$cos\theta = sin\beta\ cos\Sigma + cos\beta\ cos\gamma\ sin\Sigma \tag{16}$$

It is now required to use this knowledge of geometry and transpose the already known radiation values perpendicular to the sunrays (E_b) and on the horizontal plane (E_d) on to a vertical surface. As discussed in the beginning of Section 4.1, solar radiation at any point is the summation of its three components: direct, diffuse and reflected. For an arbitrary oriented surface, the direct component of radiation $E_{t,b}$ is calculated using simple geometry:

$$E_{t,b} = E_b\ cos\theta \tag{17}$$

The diffuse part of radiation for a vertical surface is calculated by equation 18 (Stephenson, 1965; Threlkeld, 1963):

$$E_{t,d} = E_d \max(0.45, 0.313\ cos^2\theta + 0.437\ cos\theta + 0.55) \quad (18)$$

Reflected part of radiation for a surface with angle of tilt Σ can be calculated by (ASHRAE Standard Committee, 2013):

$$E_{t,r} = \rho_g \frac{1 - cos\Sigma}{2} (E_b\ sin\beta + E_d) \quad (19)$$

here, ρ_g corresponds to reflectance by the ground, and is commonly taken as 0.2 for typical ground surfaces, like dry ground/grassland or concrete surface. For a more specific type of reflecting surface, literature can be referenced (Thevenard & Haddad, 2006).

Finally, the total radiation from the sun on a surface is obtained by the summation of equations 17, 18 and 19.

To determine solar radiation on a vertical surface, all the above calculations are performed for Houston, TX, USA for 365 days of a year and for every hour of the day, from sunrise to sunset. The number of hours for which sunshine is received each day differs, but for easier comprehension, let's assume it to be 10 hours, according to which, 3,650 different values of radiation are obtained.

In addition to the time variation, radiation received by a surface would also vary by changing surface azimuth angle ψ. Thus, to account for this change, radiation intensity is calculated for 16 different azimuth angles, corresponding to 16 cardinal directions as shown in Figure 6. This yields 3,650*16 values of radiation intensity. Let this collection of values be called Set 1.

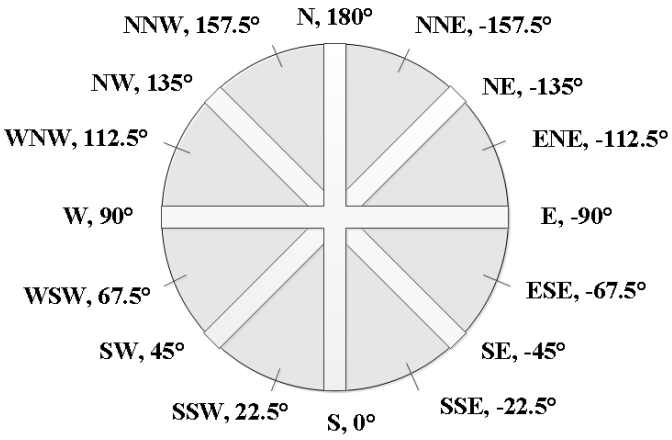

Figure 6. Different values of surface azimuth angle ψ considered for a vertical surface

To understand the magnitude of impact caused by inclusion of solar radiation to the design of flare system, maximum value of radiation intensity that can occur on a vertical surface at any time is calculated. For this case, the surface azimuth angle does not stay constant, but changes continuously with the Sun, from East to West. This set of 3,650 values capture the maximum solar radiation on a vertical plane. This collection of values is referred as Set 2.

Statistical analysis in the form of frequency distribution is carried out for both Set 1 and Set 2 values so that a certain value can be used as the contribution of radiation from the Sun to the total radiation level experienced. Further, the value is used as a parameter in PHAST calculations explained in the following section.

4.2 THERMAL RADIATION FROM FLARE

Combustion of hydrocarbon gases is a complex phenomenon and representation of the radiation emitted from it is not straightforward. Nevertheless, there is an

abundance of models to calculate thermal radiation emitted by a fire. The radiation models can be one of the following three types:

a. Semi-empirical models
b. Field models
c. Integral models

Field models are computationally intense as they are based upon solution of Navier-Stokes equations averaged over time for momentum and mass. Semi-empirical models are based on experimental results and are much simpler than field models. Integral models are a middle ground between the other two models.

For evaluating hazards in a facility, semi-empirical methods provide reasonable accuracy and are used in this study. Thermal radiation from flare is calculated by using a hazard consequence modeling software PHAST developed by DNV-GL. It has an in-built Radiation (RADS) jet flame model to predict thermal radiation intensity. It assumes the fire geometry to be a conical frustum. The model is verified and validated against experimental testing done by Chamberlain (1987) and Bennett *et al* (1991). Flare modeling in PHAST is done as a "stand-alone" equipment item and the scenario is that of a jet fire. The input to the scenario is mentioned below in Table 3 and is arranged according to the tabs that appear when inputting data.

Table 3. Input data for PHAST simulation

S. No.	Tab	Group	Field	Value
1.	Jet fire	Jet fire model	Jet fire model type	Cone model
2.		Release location	Elevation of discharge point	25 m
3.		Release characteristics	jet velocity	55 m/s
4.			Mass discharge rate	12.6 kg/s
5.			Two-phase release	[unchecked]
6.			Post-expansion jet temperature	148.85 °C
7.	Cone model data	Cone model data	Inclination of jet from horizontal	45°
8.	Radiation calculations	Type of radiation results required	Radiation at a point	[unchecked]
9.			Radiation vs distance	[checked]
10.			Radiation ellipse	[checked]
11.			Radiation contours	[unchecked]
12.	Radiation vs distance	Transect	Maximum distance	300 m
13.			Angle from release direction	0°
14.			Height above origin	0 m
15.		Observer	Fixed inclination	[unchecked]
16.			Fixed orientation	[unchecked]
17.	Radiation ellipse	Ellipse	Ellipse type required	Incident radiation
18.			Specified radiation intensity	1.58 and 4.73 kW/m^2 (in different simulations)
19.		Observer	Fixed inclination	[unchecked]

For the study, radiation level of 4.73 kW/m^2 and 1.58 kW/m^2 as mentioned in Table 1 are analyzed, since solar radiation is expected to be very less to make a difference in the calculations for the rest of higher radiation levels.

Sample calculations from the Appendix of API 521 were adopted to be used for flare specification in terms of mass discharge rate, flare temperature and average molecular mass. A mixture of light hydrocarbons was assumed with average molar mass of 46.1. Velocity was calculated based on Mach number of 0.2, which is an acceptable design value for normal flow of gas from flare.

Height of the flare was assumed to be 25 m, which falls in the typical range of height of the flare of 10-100 m. Some other inputs required before running the simulation are presented in Table 4.

Table 4. Further input data for PHAST

Material (mol fraction)	Methane (0.08)
	Propane (0.62)
	n-Butane (0.30)
Wind Speed	5 m/s
Pasquill Stability	D
Solar Radiation Intensity	0.85 kW/m^2

4.3 EFFECT OF SOLAR RADIATION ADDITION

This section describes the procedure utilized in quantitatively measuring the effect of including solar radiation in thermal radiation calculations by examining the following factors:

4.3.1 EFFECT DISTANCE FROM THE FLARE BASE

Effect distance is the distance at the ground level from the base of the flare in the downwind direction where a particular radiation level is experienced. Effect zone is the circular area with its center as the flare base and the radius as the effect distance. Inside this zone, the thermal radiation will exceed that particular level for the weather conditions assumed and for any wind direction. Effect distance and the zone increases on considering solar radiation for the radiation level of 4.73 kW/m^2 and 1.58 kW/m^2. This depicts how much under-predicted the effect distance and hence the effect zone can be when neglecting solar radiation.

4.3.2 HEIGHT OF FLARE STACK AND CORRESPONDING COST

If the facility layout is such that on considering solar radiation, the increased size of the effect zone hinders with the placement of critical equipment/units, or if the available space is limited, flare stack can be raised to an extent that the effect distance remains unaltered even after the inclusion of solar radiation. This factor helps to determine how high of a cost will have to be incurred for raising the flare stack in order to restrict the effect zone to what it was when solar radiation was neglected. Equipment cost of a self-supported flare can be estimated using equation 20 (Mussatti, Srivastava, Hemmer, & Strait, 2002).

$$C = (9.14D + 0.749L + 78)^2 \quad (20)$$

where cost, C is in dollars

diameter of flare tip, D in inches

length, L of flare stack in feet

It is a representation of the cost of the stack along with some of its ancillary equipment. Self-supported flare is designed for stack heights falling roughly in the range of 30-250 feet and the cost equation is developed for flare-tip diameter of 1-60 in. It has to be borne in mind that the cost equation is developed using various quotes provided by vendors and is believed to have an accuracy of ±30%.

4.3.3 PROBABILITY OF INJURY/FATALITY

To examine the extent of consequence of solar radiation contribution to thermal radiation onto the personnel present in the vicinity of the flare stack, the probability of them getting injured/killed is studied. The study is performed using probit equations. It is believed that this statistical model is helpful both in the design phase and the risk assessment phase of the flare system. However, probit equations prediction is not free of uncertainties, one of the reasons being unpredictability of human reaction behavior to radiation from fire.

TNO Green Book presents equation 21 and equation 22 for probability of fatality and 2nd degree burns respectively, in terms of probit (Bosch & Twilt, 1992). The probit can then be converted to percentage by using the erf function shown in equation 23 (De Haag & Ale, 2005). The probits are based on the work done by Tsao and Perry (1979). They made adjustment to probit based on nuclear explosion data.

$$Probit_{lethality} = 2.56 \ln\left(I^{\frac{4}{3}}\mathrm{t}\right) - 36.38 \quad (21)$$

$$Probit_{2^0 burn} = 3.0186 \ln\left(I^{\frac{4}{3}}\mathrm{t}\right) - 43.14 \quad (22)$$

where,

time of exposure, t is in seconds

radiation intensity, I is in W/m^2

$$Probability = 0.5\left[erf\left(\frac{Probit - 5}{\sqrt{2}}\right) + 1\right] \quad (23)$$

where,

$$\mathrm{erf(t)} = \frac{2}{\sqrt{\pi}}\int_0^t e^{-x^2} dx \quad (24)$$

The fatality probit developed by Lees is presented in equation 25 (Lees, 1994). In the development of this probit, the progress made in medical treatment of burn injuries is taken into account among other factors and the results obtained from the probit somewhat differ from those obtained through TNO probit.

$$Probit_{lethality} = 1.99 \ln\left(\frac{I^{\frac{4}{3}}\mathrm{t}\emptyset}{10{,}000}\right) - 10.7 \quad (25)$$

where, Φ is the clothing factor, φ = 0.5 in presence of clothing, and φ = 1 in absence of clothing

Clothing can provide protection to bare skin from thermal radiation effects considerably, if not ignited. The ignition of cloth takes place only at higher levels of radiation, higher

than 4.73 kW/m^2 and 1.58 kW/m^2 levels that are considered here for the study. Therefore, while calculating the probits, protection provided by clothing should be considered.

5 RESULTS AND DISCUSSION

5.1 SOLAR RADIATION

The analysis presented here has been performed for four different locations namely: Brisbane (Australia), Edinburgh (Scotland), Houston (TX, USA) and Punta Arenas (Chile). These locations were chosen to represent places in different hemispheres of the world: northern, southern, eastern and western. For brevity and to avoid repeatability, the results presented here are for Houston, TX, USA. Results for other locations are shown in Appendix A.

5.1.1 SOLAR RADIATION WITH DIFFERENT ORIENTATION OF A VERTICAL SURFACE

As discussed in Section 4.1.3, radiation intensity on a surface from the Sun changes with the orientation of the surface. Personnel present near the flare, while standing vertically, can be facing any direction. To capture this change along with the change caused by time, radiation values are calculated for 16 different geographical directions corresponding to different surface azimuth angles, ψ. Values for four of those directions are shown in Figure 7, Figure 8, Figure 9 and Figure 10. All these figures show the variation of solar radiation with time of the day when sunshine is received, roughly from 0600 hrs. to 1900 hrs. Also, the different curves represent the variation in radiation with different days of the year. Only four days out of 365 are illustrated, the 1st day of January, April, July and October. For some figures, the solar radiation value for hotter months is lesser, which does not seem intuitive. This is due to the altitude angle

being higher in summer which causes reduction in the value of direct solar radiation on a vertical surface.

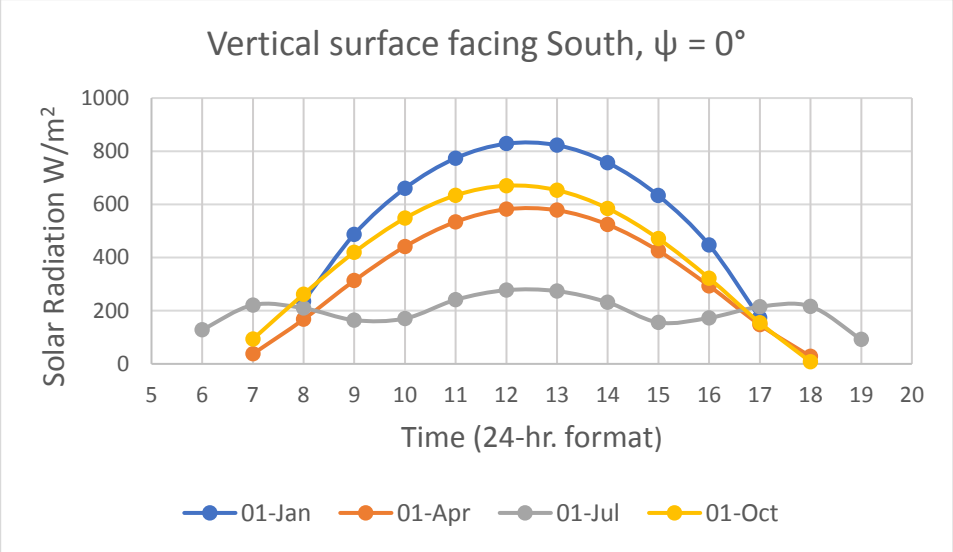

Figure 7. Solar radiation on a vertical surface facing South vs. time for different days of the year

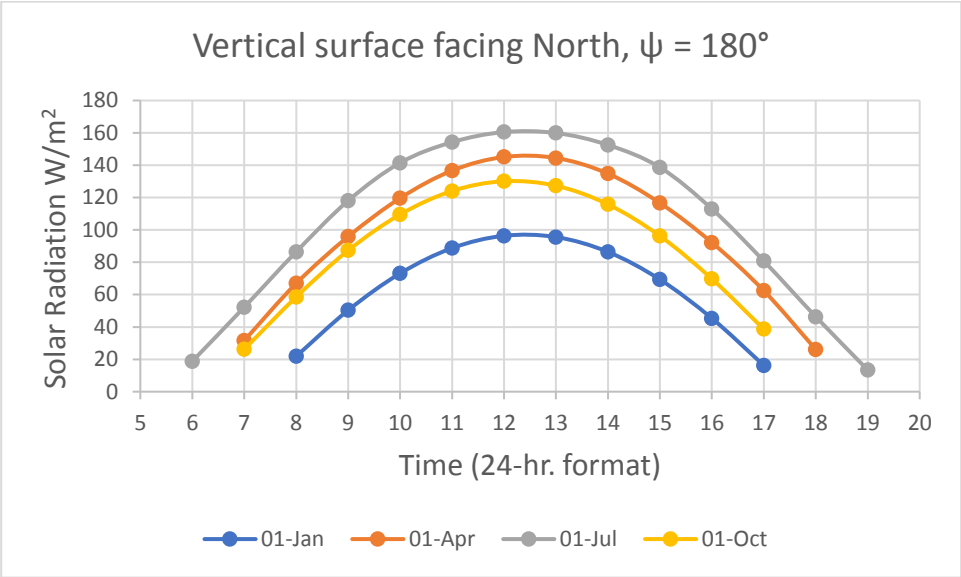

Figure 8. Solar radiation on a vertical surface facing North vs. time for different days of the year

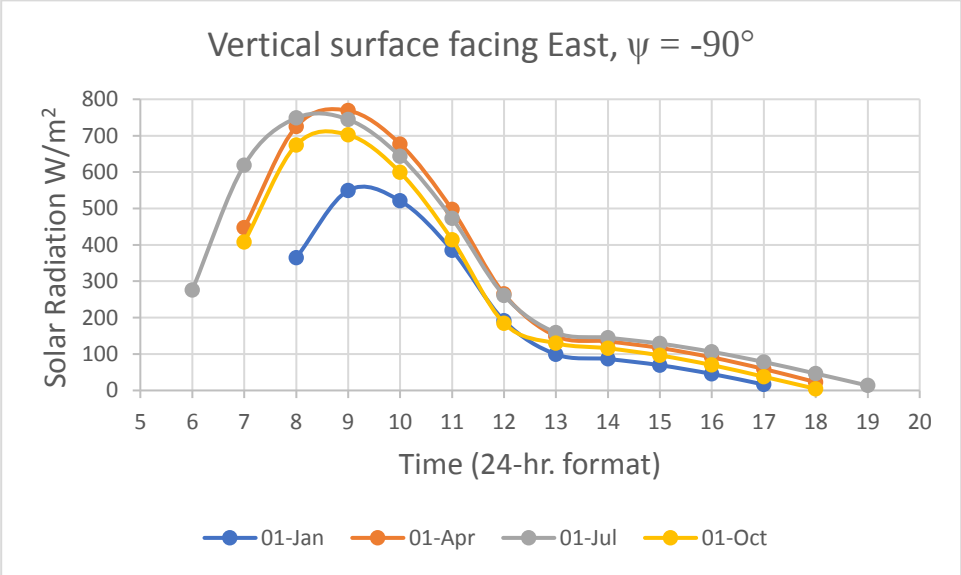

Figure 9. Solar radiation on a vertical surface facing East vs. time for different days of the year

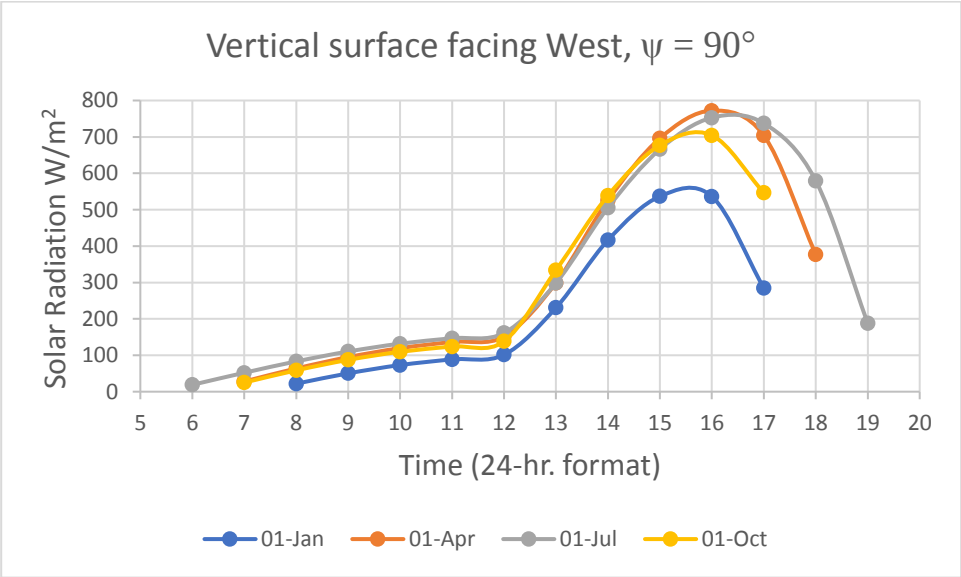

Figure 10. Solar radiation on a vertical surface facing West vs. time for different days of the year

To understand the spread of solar radiation values, the frequency distribution of Set 1 values mentioned in Section 4.1.3 is shown in Figure 11. These values correspond to surfaces facing 16 different directions. For a surface to experience higher radiation, it will have to directly face the sun, which does not have a high probability. That is the reason of frequency being higher for lower values of radiation as depicted in Figure 11.

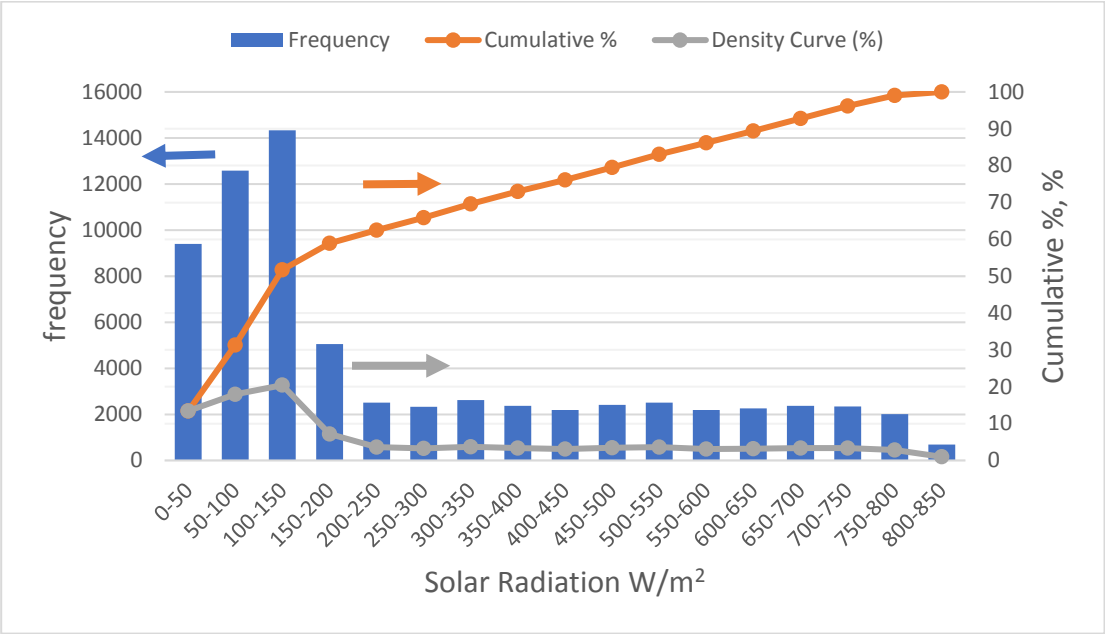

Figure 11. Frequency distribution for solar radiation values for different time, orientation

5.1.2 MAXIMUM SOLAR RADIATION

The radiation intensity in Figure 11 varies widely, from 0-850 W/m^2. A singular value of solar radiation to be added to thermal radiation from the flare must be suggested to calculate total radiation intensity received. To begin with, the maximum values of solar radiation (at different times) that can be experienced on a vertical surface, termed as Set 2 in Section 4.1.3, are determined, and shown in Figure 12. To study the outcome causing highest impact on the design of flare, the maximum value of solar radiation is considered. This approach will provide a conservative estimate.

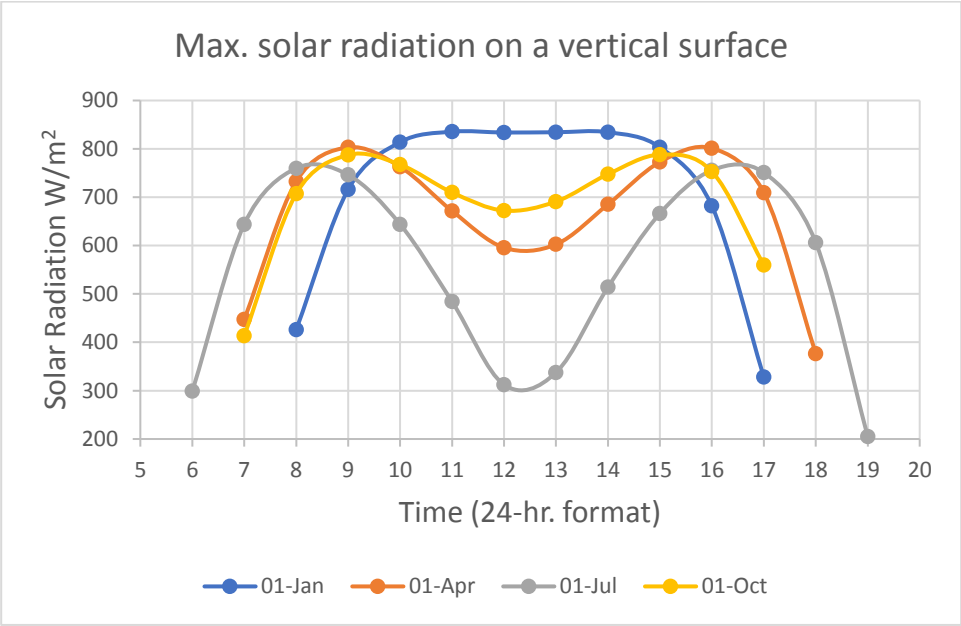

Figure 12. Maximum solar radiation on a vertical surface vs. time for different days of the year

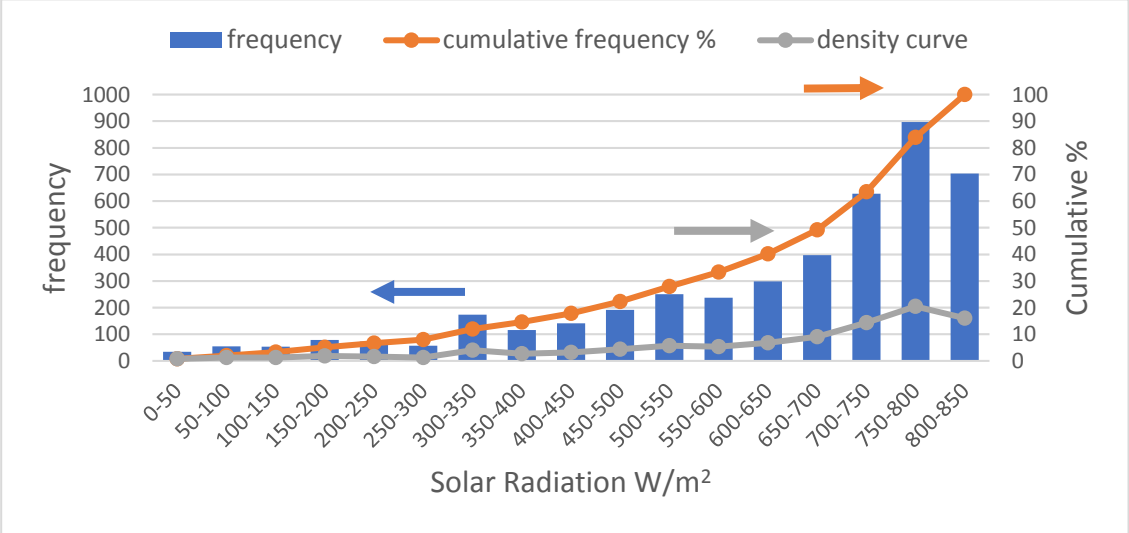

Figure 13. Frequency distribution for maximum solar radiation, for different time

To understand the spread of maximum solar radiation values, the frequency distribution of Set 2 values is shown in Figure 13. The same data is also presented in Table 5. Set 2 is a subset of Set 1. The frequency of higher values of radiation is higher because of Set 2 inherently containing all the maximum values of radiation occurring at different times of the day.

Table 5. Frequency distribution table for maximum solar radiation at different time

solar rad. (W/m^2)	frequency	frequency %	cumulative frequency %
0-50	34	0.78	0.78
50-100	55	1.25	2.03
100-150	54	1.23	3.26
150-200	79	1.80	5.06
200-250	73	1.66	6.72
250-300	57	1.30	8.02
300-350	174	3.97	11.99
350-400	116	2.64	14.63
400-450	141	3.21	17.85
450-500	192	4.38	22.22
500-550	251	5.72	27.95
550-600	237	5.40	33.35
600-650	298	6.79	40.14
650-700	397	9.05	49.19
700-750	628	14.32	63.51
750-800	897	20.45	83.95
800-850	704	16.05	100.00

As shown in Table 5, the maximum frequency of solar radiation values is for the range of 750-800 W/m^2. 800-850 W/m^2 is also very close, with frequency percent of 16%. Thus, a conservative value of 850 W/m^2 is chosen to be the contribution to the total radiation from the Sun. The same value can be taken for other places, Punta Arenas, Edinburgh and Brisbane. Of course, the frequency of solar radiation values is not same for these places, but that does not cause variation in picking the value of 850 W/m^2. The results for other locations are shown in Appendix A.

5.2 TOTAL THERMAL RADIATION

Radiation contribution from the Sun, as estimated in Section 5.1.2, is used as an input in the radiation model of PHAST. Intensity radii and size of effect zone are used to compare the consequence modeling results of the two cases of considering/not considering solar radiation while calculating incident radiation.

As mentioned in Section 4.2, the incident radiation level of 4.73 kW/m^2 and 1.58 kW/m^2 are studied to compare the consequence analysis performed.

5.2.1 INTENSITY RADII AND EFFECT ZONE

Figure 14 and Figure 15 show the radiation ellipse (solid curve) and the effect zone (dotted curve) for radiation level of 4.73 kW/m^2. The same is listed in Table 6 for both radiation levels of 4.73 kW/m^2 and 1.58 kW/m^2.

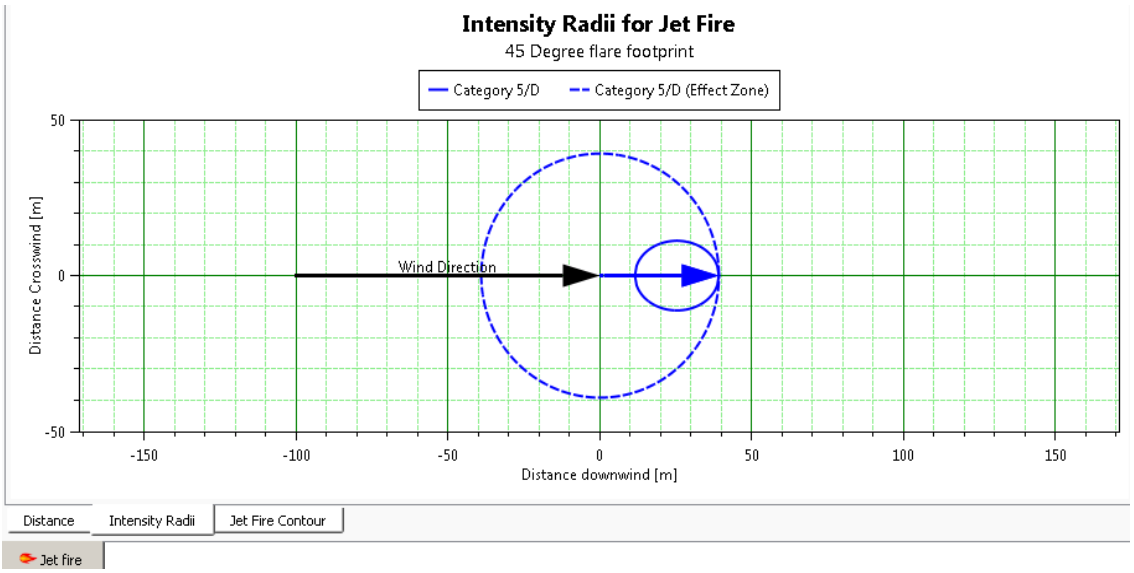

Figure 14. Radiation ellipse and effect zone discounting solar radiation

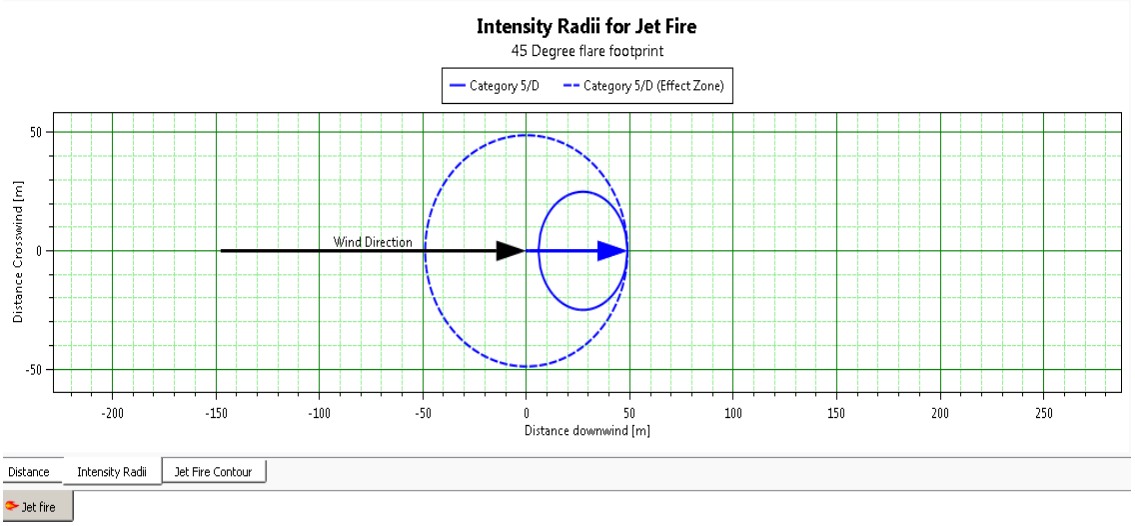

Figure 15. Radiation ellipse and effect zone considering solar radiation

Table 6. Effect distance when considering or discounting solar radiation contribution

Solar radiation of 850 W/m^2	w/o solar radiation	w/ solar radiation	% increase
Effect distance for 4.73 kW/m^2	39 m	50 m	28%
Effect distance for 1.58 kW/m^2	85 m	127 m	49%

The change in effect distance is much higher for the lower radiation level of 1.58 kW/m^2. This is because radiation falls rapidly with increase in the distance away from the flare. This can be illustrated by Figure 16 which depicts change in the radiation intensity experienced at the ground with increasing distance in the downwind direction from the base of the flare.

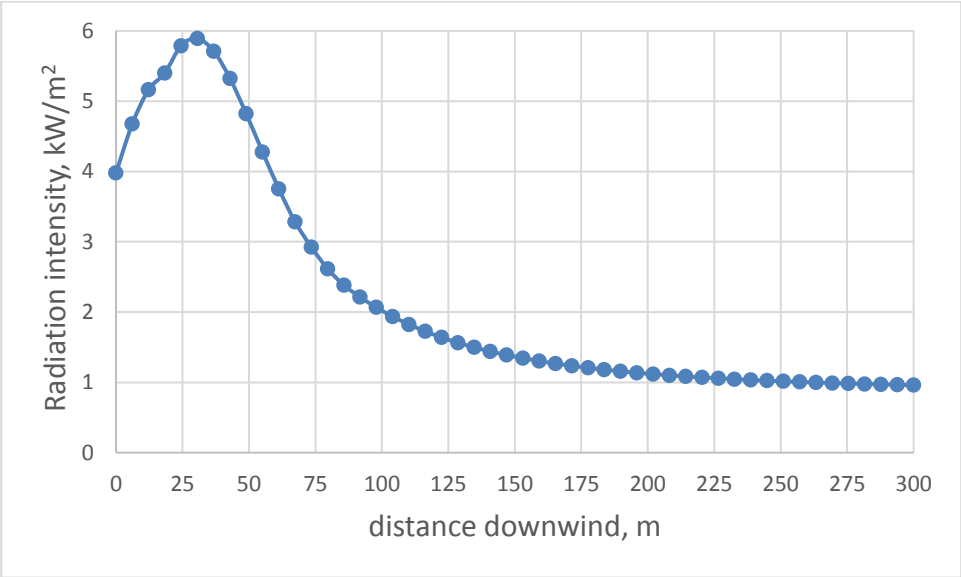

Figure 16. Total radiation intensity on the ground vs. distance downwind from the flare base

5.2.2 FLARE HEIGHT

The outcome of considering solar radiation can also be studied by maintaining the effect distance constant to the case when solar radiation is discounted, and increasing the flare stack height, such that the radiation level of 4.73 kW/m^2 and 1.58 kW/m^2 is still existent at the same distance from the flare. The increase in the stack height is shown in Table 7. Subsequently, this will translate into an increment in the cost of the flare, which is also tabulated.

Table 7. Effect of considering solar radiation contribution on flare height and its corresponding cost

	Stack height to meet 4.73 kW/m^2 level	Cost of self-supported stack for 4.73 kW/m^2 level	Stack height to meet 1.58 kW/m^2 level	Cost of self-supported stack for 1.58 kW/m^2 level
W/o solar radiation	25 m	$94,399	25 m	$94,399
W/ solar radiation	30 m	$102,100	80 m	$195,716
% increase	20 %	8 %	220 %	107 %

The increase in the cost of flare is not very high for meeting the radiation level of 4.73 kW/m^2, but it more than doubles for meeting radiation criteria for 1.58 kW/m^2 level. Before suggesting investing a huge sum of money, further analysis is conducted to make sure such a change would make the facility safer in terms of risk associated with exposure to thermal radiation.

5.2.3 RISK ASSESSMENT

Probit equations introduced in Section 4.3.3 are used to compare the two cases of discounting or considering solar radiation (SR) contribution. As per the probit equation 25 by Lees, probability of fatality for the radiation level of 4.73 kW/m^2 (radiation level without addition of solar radiation) and level of 5.58 kW/m^2 (radiation level after addition of solar radiation of 850 W/m^2) for the exposure time of two and three minutes is shown in Table 8 (Lees, 1994). Two and three minutes of exposure was chosen based on the guideline of API 521 as mentioned in Table 1. The change in the probability of

fatal injury does not change at all or changes negligibly upon consideration of solar radiation contribution.

Table 8. Probability of fatality per Lees probit equation for radiation level of 4.73 kW/m^2 (with or without SR)

	q, W/m^2	t, s	Probit	Fatal probability
no SR	4730	120	1.57	0.00
SR=850 W/m^2	5580	120	2.00	0.00
no SR	4730	180	2.38	0.00
SR=850 W/m^2	5580	180	2.82	0.01

Similar analysis as above is repeated using probit equation of the TNO Green Book and shown in Table 9. The fatality obtained by the probit equation 21 is reduced by multiplying by a factor of 0.14 to account for the protective effect of clothing (Bosch & Twilt, 1992).

Table 9. Probability of fatality per Green Book probit equation for radiation level of 4.73 kW/m^2 (with or without SR)

--	q, W/m^2	t, s	Probit	Fatal probability (no clothing)	Fatal probability (with clothing)
no SR	4730	120	4.76	0.40	0.06

Table 9. Continued

	q, W/m^2	t, s	Probit	Fatal probability (no clothing)	Fatal probability (with clothing)
SR=850 W/m^2	5580	120	5.32	0.63	0.09
no SR	4730	180	5.80	0.79	0.11
SR=850 W/m^2	5580	180	6.36	0.91	0.13

Table 10. Probability of 2nd degree burn per Green Book probit equation for radiation level of 4.73 kW/m^2 (with or without SR)

	q, W/m^2	t, s	Probit	Probability for 2nd degree burn (no clothing)	Probability for 2nd degree burn (with clothing)
no SR	4730	120	5.37	0.64	0.09
SR=850 W/m^2	5580	120	6.03	0.85	0.12
no SR	4730	180	6.59	0.94	0.13
SR=850 W/m^2	5580	180	7.26	0.98	0.14

The increase in the probability of a fatal injury for radiation level of 4.73 kW/m^2 (from no SR to considering SR = 850 W/m^2) is not very significant. It increases from 6% to 9% for 120 s. of exposure, and from 11% to 13% for 180 s. of exposure. Similarly, the probability of 2nd degree burns, as shown in Table 10, has not notably increased. It should be noted that these fatality/injury probability numbers are further multiplied to

other probabilities, like probability of a person present in the concerned area and probability of the wind speed prevailing at the time. when performing a full-blown risk assessment. Therefore, the impact to the sustained risk by disregarding solar radiation contribution would be diminished further.

The probit equations presented in the TNO book is based on the work done by Tsao and Perry (Tsao & Perry, 1979). They made modifications to the vulnerability model developed by Eisenberg *et al* who put forward the probit on the basis of radiation injuries caused by the nuclear explosions (Eisenberg, Lynch, & Breeding, 1975). Although, Tsao and Perry made adjustment to their model to account for the difference in extent of injuries caused by infrared radiation (from hydrocarbon fire) rather than UV and visible radiation (from nuclear explosions), some other conditions and assumptions remain the same. For example, the treatment of burn injuries and fatalities have improved significantly since 1975. Also, the probit results are based on the injuries caused to all the age groups, including children and older people. Both these groups are more vulnerable to burn injury in comparison to the people belonging to the typical working-age class. In addition, TNO considers protection provided by clothing based on the average population statistics of Netherlands, which again includes younger and older population. Hence, all these attributes make the TNO probit equation conservative in predicting thermal radiation effects on personnel.

On the other hand, Lees probit equation incorporates more recent advancements in medical treatment and knowledge of intensity of the burns (Lees, 1994). The population considered also lies in the age category of 10-69 years, thus discounting the

more vulnerable categories of children and older people. Hence, the Lees probit equation seems to be a better representation of the probability of fatality from thermal radiation, shown in Table 8.

Therefore, for the suggested level of 4.73 kW/m^2 by API 521, for which emergency action may be performed by personnel clad in proper clothing lasting about 2-3 minutes, a disregard for solar radiation does not significantly alter the probability of fatality. Also, the probability of 2nd degree burns as shown in Table 10 does not increase by a considerable extent.

Similar analysis is also performed for the radiation level of 1.58 kW/m^2, for which API 521 suggests that the personnel can be present in that area for extended periods of time. However, using Lees probit for an exposure time of 1 hr. and 2 hrs. yields very high probability of fatality, as shown in Table 11, which seems to be unlikely.

Table 11. Probability of fatality per Lees probit equation for radiation level of 1.58 kW/m^2 (with or without SR)

	q, W/m^2	t, s	Probit	Fatal probability
no SR	1580	3600	5.43	0.67
SR=850 W/m^2	2430	3600	6.57	0.94
no SR	1580	7200	6.81	0.96
SR=850 W/m^2	2430	7200	7.95	0.99

It has been discussed previously that using probit relations at extremes can result in overly conservative estimates (Daycock & Rew, 2000). A very high exposure time will result in a high thermal dose (dose = $q^{4/3}t$) even when the radiation intensity is low, as shown in the case of radiation level of 1.58 kW/m^2. Moreover, the experiments/data used to develop these probit equations have exposure time of a few seconds, and not hours. Thus, the conclusion drawn from probit for extended exposure time is not reliable.

Since, radiation level of 1.58 kW/m^2 is too low to cause fatality, another method to measure heat stress caused by continuous exposure can be utilized: an index for the assessment of hot environments. One such empirical index is Wet Bulb Globe Temperature (WBGT) which is extensively used and is also presented in ISO Standard 7243 (International Standards Organization, 1982). WBGT is measured using instrument on site, but can also be calculated fairly accurately using available weather data as done by Liljegren *et al* (2008). Software[1] has been developed which has automated the calculations and only requires weather data as input (Liljegren, 2008). Input as shown in Table 12 was used for Houston, TX when considering solar radiation in the calculations.

[1] Copyright © 2008, UChicago Argonne LLC, All Rights Reserved, Wet Bulb Globe Temperature (WBGT) Version 1.2, Author: James Liljegren, Argonne National Laboratory, DIS Divison.

Table 12. Input and output in software used to calculate WBGT, considering solar radiation

Air temperature	28.9 °C
Solar irradiance	850 W/m^2
Wind speed	5 m/s
Relative humidity	50%
Atmospheric pressure	1009.4 millibar
WBGT obtained	26.3 °C

The air temperature considered is the maximum average temperature for Houston (ASHRAE Standard Committee, 2013).

Since clothing restricts evaporative cooling of the body, and tends to increase core body temperature, effective WBGT ($WBGT_{eff}$) is obtained by adding clothing adjustment factor (CAF) to the WBGT, both expressed in degree Celsius. Refer to Table 13 for the same. (American Conference of Governmental Industrial Hygienists, 2017). For this study, clothing is taken as normal cotton work clothes, for which $WBGT_{eff}$ = WBGT.

Table 13. Clothing adjustment factor to WBGT

Clothing Worn	CAF
Work clothes (long sleeves and pants). Examples: Standard cotton shirt/pants.	0
Coveralls (w/only underwear underneath). Examples: Cotton or light polyester material.	0
Double-layer woven clothing.	3
SMS Polypropylene Coveralls	0.5
Polyolefin coveralls. Examples: Micro-porous fabric (e.g., Tyvek™).	1
Limited-use vapor-barrier coveralls. Examples: Encapsulating suits, whole-body chemical protective suites, firefighter turn-out gear.	11

Metabolic rate (MR) of personnel should also be known to calculate heat stress. It can be estimated by using equation 26 (American Conference of Governmental Industrial Hygienists, 2017). Body weight is assumed to be 70 kg for simplification and Table 14 is referred to know work expectation (in Watts) (American Conference of Governmental Industrial Hygienists, 2017). Moderate work expectation from the worker is assumed, which translates to 300 W. Threshold limit values (TLV) for different types of workload are suggested in Table 15, and if $WBGT_{eff}$ exceeds the TLV, worker is believed to be under risk due to heat stress and exhaustion (American Conference of Governmental Industrial Hygienists, 2017). Nevertheless, it should be kept in mind that TLV is just a screening tool. When $WBGT_{eff}$ does exceed TLV, further detailed analysis, *e.g.*, physiological monitoring should be performed.

$$MR = \ Work\ expectation\ (in\ Watts) \times \frac{worker\ body\ weight\ (in\ kg)}{70\ kg} \quad (26)$$

Table 14. Work expectation in terms of different work category

Work Category	Work expectation (Watts)	Examples
Rest	115	Sitting
Light	180	Sitting, standing, light arm/hand work and occasional walking
Moderate	300	Normal walking, moderate lifting
Heavy	415	Heavy material handling, walking at a fast pace
Very Heavy	520	Pick and shovel work

Table 15. Threshold limit Values (TLV) for different work load and different work/rest regime

% Work	Workload/ Work expectation			
	Light	Moderate	Heavy	Very Heavy
75 to 100% (Continuous)	31.0°C	28.0°C	N/A	N/A
50 to 75%	31.0°C	29.0°C	27.5°C	N/A
25 to 50%	32.0°C	30.0°C	29.0°C	28.0°C
0 to 25%	32.5°C	31.5°C	30.5°C	30.0°C

Even for continuous work, and moderate workload as assumed, TLV is 28 °C from Table 15, and $WBGT_{eff}$ = 26.3 °C from Table 12, which does not exceed TLV. Therefore, even with considering solar radiation, workers are at a significantly low risk of heat stress.

6 CONCLUSIONS AND RECOMMENDATIONS

The study carried out here tries to quantitatively address the variation of either considering or disregarding solar radiation when designing flare based on allowed thermal radiation levels on the ground. Since, the objective of the study was to develop a framework that helps in making the most suitable decision for the specific facility, the conclusions drawn here are relevant when the same data and assumptions hold true at the site. Nevertheless, the framework can still be applied in other cases, and conclusions drawn based on results thus obtained.

Radiation level of 4.73 kW/m^2 and 1.58 kW/m^2 are studied for this assessment, and the two cases of zero solar radiation (SR) contribution and solar radiation contribution of 850 W/ m^2 are compared. It is worth noting that 850 W/m^2 is the maximum value of solar radiation that may exist at any time on a vertical plane.

- For radiation level of 4.73 kW/m^2, consideration of SR demands either a 28% increase in the effect distance as shown in Table 6, which translates to a 64% increase in the effect zone, or an increase in flare height causing the flare cost to increase by 8% as shown in Table 7. However, on doing so, the risk to personnel in terms of reduction of the probability of death/second degree burn shown in Table 8 and Table 10 is not significant.
- For radiation level of 1.58 kW/m^2, consideration of SR demands either a 49% increase in the effect distance as shown in Table 6, which translates to a 122% increase in the effect zone, or an increase in flare height causing the flare cost to

increase by 107% as shown in Table 7. The increase in design values is too high. The decision of accounting for SR should not be made without assessing the actual outcome of neglecting SR. This is done by estimating heat stress experienced by a worker. Since WBGT, which is a heat index extensively used, calculated and shown in Table 12, is below the TLV discussed in Table 15, SR can be safely neglected without compromising the safety of the workers exposed. That being said, WBGT did not exceed TLV for the given weather data, where air temperature is assumed to be the maximum average monthly temperature for Houston, TX. It is possible that some days are hotter and WBGT exceeds TLV on those days. In that case, exercising general controls at the site will be much more feasible in maintaining safe working environment in contrast to designing the flare system with the absolute worst conditions which have a very low probability of occurrence and still do not lend notable reduction in the risk level. General controls include, an appropriate work/rest regime where workers take few minutes break during every hour, physiological monitoring of the workers and an improved awareness about the symptoms to look out that suggest heat exhaustion.

After carrying the analysis explained in this study, it can be concluded that solar radiation contribution can be discounted while designing flare based on 4.73 kW/m^2 and 1.58 kW/m^2 radiation level. Even after taking the highest value of solar radiation, the apparent risk reduction is not remarkable to justify the immense increase in design factors. When designing a flare, this can further be confirmed by using the

conditional probability data for the quantitative risk assessment (QRA) performed for the flare system. QRA uses conditional probability of rest of the factors, like, weather and wind direction probability, probability of the person present in the area where particular radiation level exists. Using this information, risk posed on the facility in terms of fatalities/injuries per year can be computed and compared. For heat stress values, the data and conclusions presented in the study can further be stated with enhanced confidence by measuring WBGT with the help of meteorological data of the particular site, or better still using WBGT monitors installed on workers' bodies.

REFERENCES

American Conference of Governmental Industrial Hygienists. (2017). *TLVs and BEIs Threshold Limit Values for Chemical Substances and Physical Agents and Biological Exposure Indices*

American Petroleum Institute. (2007). API 521 Pressure-relieving and depressuring systems.

American Petroleum Institute. (2008). API 537- Flare Details for General Refinery and Petrochemical Service.

ASHRAE Standard Committee. (2013). Chapter 14: Climatic Design Information. In *ASHRAE Handbook: Fundamentals*

Bamber, J. L., & Payne, A. J. (2004). *Mass balance of the cryosphere: observations and modelling of contemporary and future changes*: Cambridge University Press.

Banerjee, K., Cheremisinoff, N. P., & Cheremisinoff, P. N. (1985). *Flare gas systems pocket handbook*: Gulf Publishing.

Baukal Jr, C. E. (2012a). The John Zink Hamworthy Combustion Handbook. In (2nd ed., Vol. 3, pp. 253). Boca Raton: CRC Press.

Baukal Jr, C. E. (2012b). The John Zink Hamworthy Combustion Handbook. In (2nd ed., Vol. 1, pp. 480-512). Boca Raton: CRC press.

Baukal Jr, C. E. (2012c). The John Zink Hamworthy Combustion Handbook. In (2nd ed., Vol. 3, pp. 251-297). Boca Raton: CRC Press.

Baukal Jr, C. E. (2012d). The John Zink Hamworthy Combustion Handbook. In (2nd ed., Vol. 1, pp. 207-225). Boca Raton: CRC press.

Bennett, J., Cowley, L., Davenport, J., & Rowson, J. (1991). Large scale natural gas and LPG jet fires final report to the CEC. *Shell report TNER, 91*.

Bosch, C. J. H. v. d., & Twilt, L. (1992). Damage caused by heat radiation. In *Methods for the determination of possible damage to people and objects resulting from releases of hazardous materials Report CPR E* (Vol. 16): TNO - The Netherlands Organisation of Applied Scientific Research.

Chamberlain, G. (1987). Developments in design methods for predicting thermal radiation from flares. *Chemical Engineering Research and Design, 65*(4), 299-309.

Cooper, P. (1969). The absorption of radiation in solar stills. *Solar energy, 12*(3), 333-346.

Daycock, J., & Rew, P. (2000). *Thermal radiation criteria for vulnerable populations*: HSE Books.

De Haag, P. U., & Ale, B. (2005). *Guidelines for Quantitative Risk Assessment: Purple Book*: Ministerie van Volkshuisvesting en Ruimtelijke Ordening (VROM).

Eisenberg, N. A., Lynch, C. J., & Breeding, R. J. (1975). *Vulnerability model. A simulation system for assessing damage resulting from marine spills*.

Gueymard, C. A. (2008). REST2: High-performance solar radiation model for cloudless-sky irradiance, illuminance, and photosynthetically active radiation–Validation with a benchmark dataset. *Solar energy, 82*(3), 272-285.

Hajek, J. D., & Ludwig, E. E. (1960). How to Design Safe Flare Stacks. *Petro/Chem Engineer, 32*(6), C31–C38.

International Standards Organization. (1982). Hot Environments- estimation of heat stress on working man based on the WBGT (Wet Bulb Globe Temperature) index ISO 7243.

Iqbal, M. (1983). *An introduction to solar radiation*. Ontario, Canada: Academic Press.

Johnson, A., Brightwell, H., & Carsley, A. (1994). A model for predicting the thermal radiation hazards from large-scale horizontally released natural gas jet fires. *Process safety and environmental protection, 72*, 157-166.

Kasten, F., & Young, A. T. (1989). Revised optical air mass tables and approximation formula. *Applied optics, 28*(22), 4735-4738.

Kreith, F., & Kreider, J. F. (1978). *Principles of solar engineering*: HemispherePub. Corp.

Lees, F. P. (1994). The assessment of major hazard: a model for fatal injury from burns. *Process safety and environmental protection, 72*(3), 127-134.

Liljegren, J. C. (2008). Wet Bulb globe Temperature (WBGT) (Version 1.2): Argonne National Laboratory, DIS Division.

Liljegren, J. C., Carhart, R. A., Lawday, P., Tschopp, S., & Sharp, R. (2008). Modeling the wet bulb globe temperature using standard meteorological measurements. *Journal of occupational and environmental hygiene, 5*(10), 645-655.

McMurray, R., Oswald, B. J., & Witheridge, R. E. (1980). *A Guide To Flare System Design, With Particular Reference To Offshore Platforms.* Paper presented at the Offshore Technology Conference.

Mussatti, D. C., Srivastava, R., Hemmer, P. M., & Strait, R. (2002). EPA air pollution control cost manual. *Air Quality Strategies and Standards Division of the Office of Air Quality Planning and Standards, US Environmental Protection Agency, Research Triangle Park, NC, 27711*.

Oenbring, P., & Sifferman, T. (1980). Flare design... are current methods too conservative. *Hydrocarbon Processing, 60*(5), 124-129.

Schwartz, R. E., & Kang, S. G. (1998). *Flare System Design- What is Important?*

Stephenson, D. G. (1965). Equations for solar heat gain through windows. *Solar energy, .9*(2), 81-86.

Thevenard, D., & Haddad, K. (2006). Ground reflectivity in the context of building energy simulation. *Energy and buildings, 38*(8), 972-980.

Threlkeld, J. L. (1963). Solar irradiation of surfaces on clear days. *ASHRAE Transactions, 69*, 24-36.

Tsao, C. K., & Perry, W. W. (1979). *Modifications to the vulnerability model: A simulation system for assessing damage resulting from marine spills* (CG-D-38-79). Retrieved from Washington, D. C. 20590.

APPENDIX

Here, the values of solar radiation existing at different times at Punta Arenas (Chile), Edinburgh (Scotland) and Brisbane (Australia) are presented in the said order. Figure 17, Figure 18 and Figure 19 show the frequency distribution of SR values in Set 1, comprising of SR values corresponding to the surface facing 16 different directions.

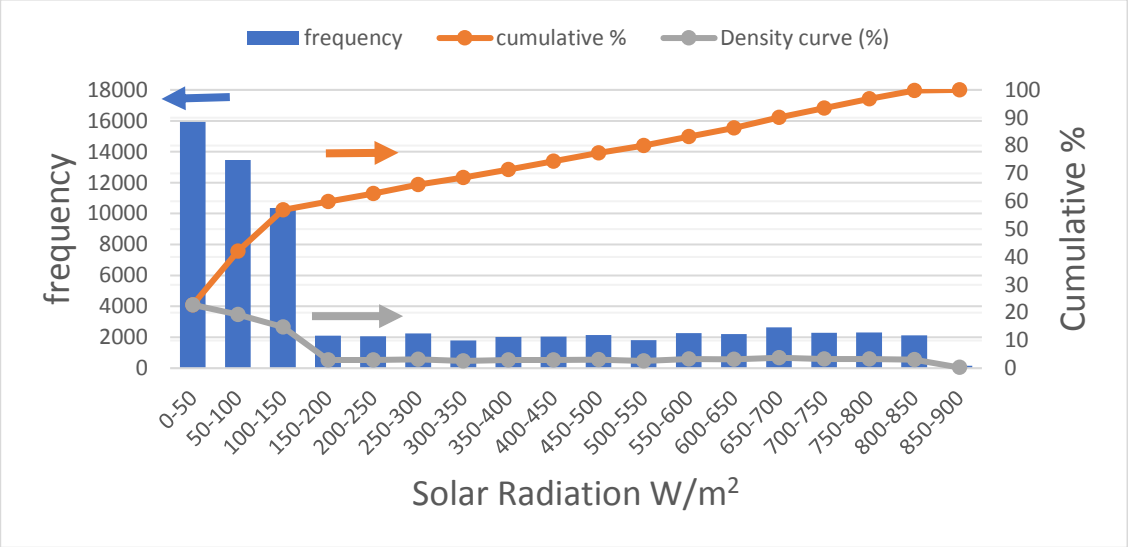

Figure 17. Frequency distribution for solar radiation values for different time, orientation for Punta Arenas, Chile

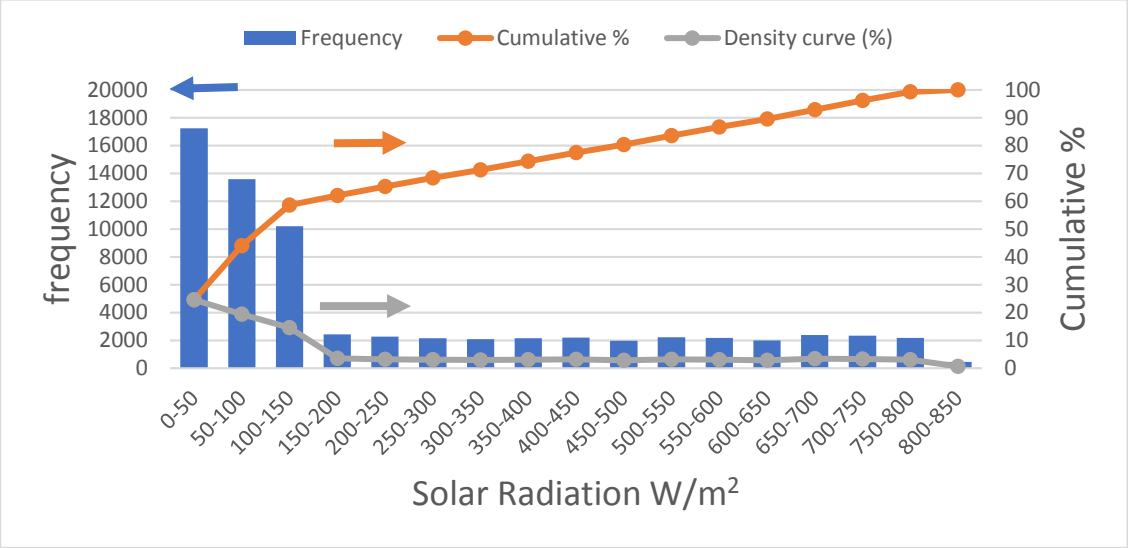

Figure 18. Frequency distribution for solar radiation values for different time, orientation for Edinburgh, Scotland

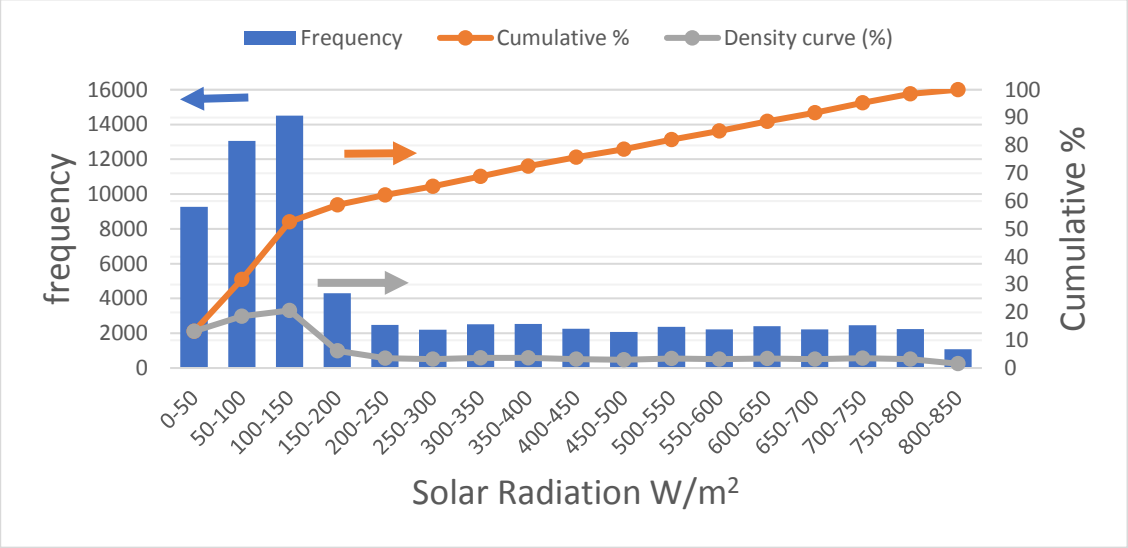

Figure 19. Frequency distribution for solar radiation values for different time, orientation for Brisbane, Australia

To adopt a more conservative approach in choosing the SR contribution, frequency distribution for Set 2 values is shown in Figure 20, Figure 21 and Figure 22 for Punta Arenas, Edinburgh and Brisbane respectively. The analysis done for picking 850 W/m^2 as SR contribution for Houston is also valid for these locations. For Punta Arenas, there are some values which are in the range of 850-900 W/m^2. 7% of the total SR values fall in the range of 850-900 W/m^2 as compared to a much higher 27% of the total SR values falling in the range of 800-850 W/m^2. Therefore, the decision of picking 850 W/m^2 as SR contribution is still justified.

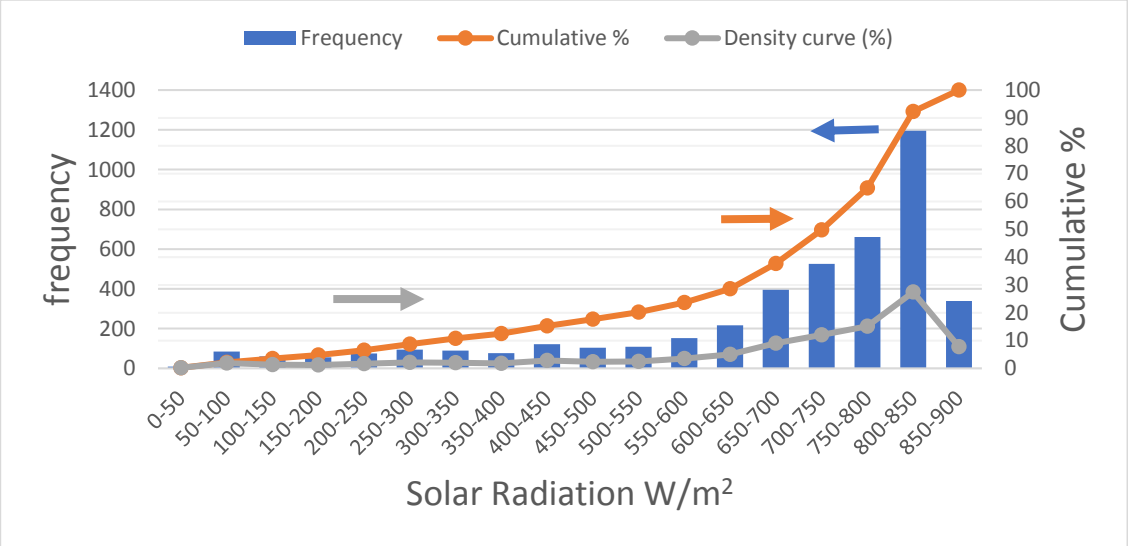

Figure 20. Frequency distribution for maximum solar radiation, for different time at Punta arenas, Chile

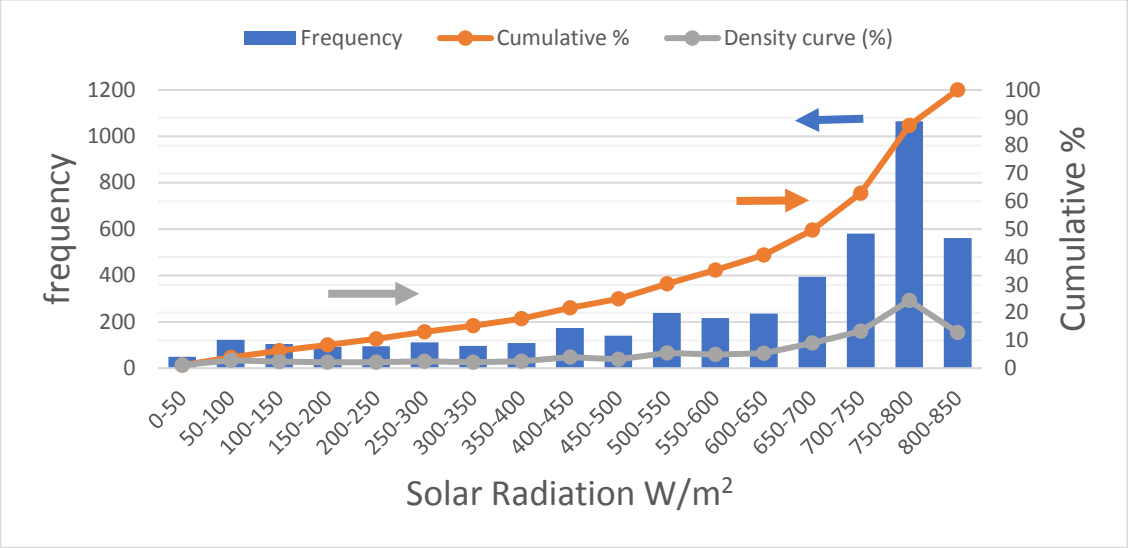

Figure 21. Frequency distribution for maximum solar radiation, for different time at Edinburgh, Scotland

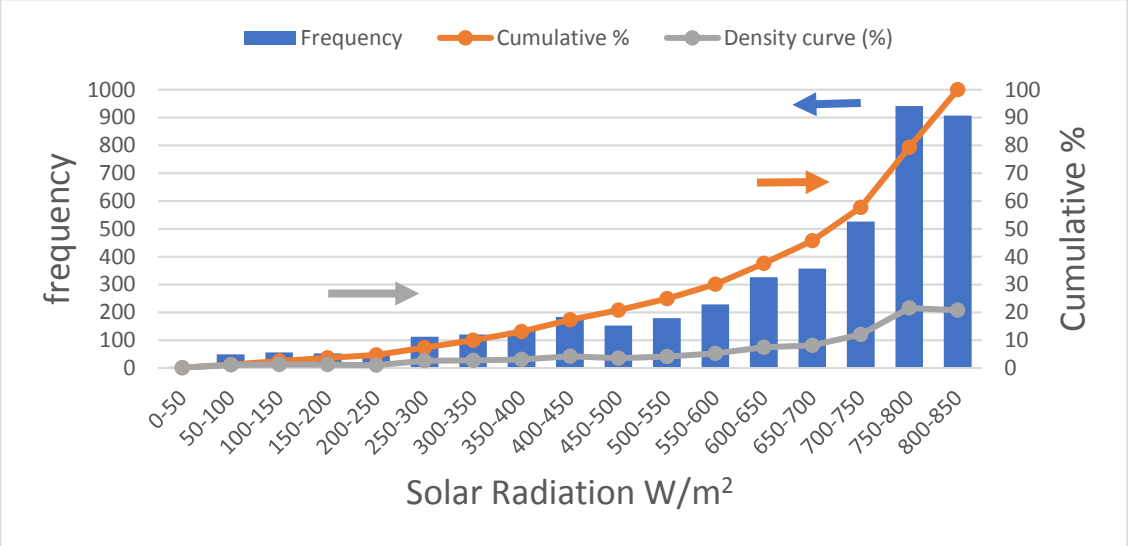

Figure 22. Frequency distribution for maximum solar radiation, for different time at Brisbane, Australia